Agricultural and Forest Meteorology 279 (2019) 107707

Contents lists available at ScienceDirect

Agricultural and Forest Meteorology

journal homepage: www.elsevier.com/locate/agrformet

Agricultural drought monitoring using European Space Agency Sentinel 3A land surface temperature and normalized difference vegetation index imageries

Xingbang Hu[a,b], Huazhong Ren[a,b,*], Kevin Tansey[c], Yitong Zheng[a,b], Darren Ghent[d], Xufang Liu[a,b], Lei Yan[a,b,*]

[a] Institute of Remote Sensing and Geographic Information System, School of Earth and Space Sciences, Peking University, Beijing 100871, China
[b] Beijing Key Lab of Spatial Information Integration and Its Application, Peking University, Beijing 100871, China
[c] Leicester Institute for Space and Earth Observation, Centre for Landscape & Climate Research, School of Geography, Geology and the Environment, University of Leicester, Leicester, UK
[d] National Centre for Earth Observation (NCEO), Earth Observation Science, Department of Physics & Astronomy, University of Leicester, UK

ARTICLE INFO

Keywords:
Agricultural drought
Sentinel 3A LST
VTCI
Drought index

ABSTRACT

Agricultural drought is one of most damaging agricultural hazards worldwide that can bring significant agricultural losses and water scarcity. The use of satellite images for monitoring agricultural drought has received increasing research attention and has also been applied at both the regional and global scales. In this paper, the land surface temperature (LST) and radiance products of the new Sentinel-3A SLSTR (sea and land surface temperature radiometer) launched by European Space Agency (ESA) are used for the first time for estimating the vegetation temperature condition index (VTCI), which in turn is used for monitoring agricultural drought in the Hetao Plain of Inner Mongolia, China. This paper initially analyzes the correlation between LST and normalized difference vegetation index (NDVI) by using time series time MODIS LST and NDVI products under different vegetation growth conditions. The findings reveal that VTCI can only be used in warm seasons (late spring and summer periods) when negative correlations between LST and NDVI are observed. Therefore, VTCI images are captured in the study area between July and August 2017 by using Sentinel-3A SLSTR LST and NDVI and are utilized for drought investigation. These images reveal that the average VTCI of the cultivated land pixels in the study area has increased from 0.4511 on July 28 to 0.5229 on August 12 before declining to 0.4710 on August 18 due to the rainfall in the first period, thereby indicating that VTCI has a timely response to rainfall. Meanwhile, cross-comparison of VTCI values from Sentinel-3A SLSTR shows high consistency in terms of spatial distribution with that estimated from EOS MODIS products. The difference between these indices ranged from −0.1 to 0.1 for most points, especially in the cultivated land cover. Overall, the findings support the use of the LST and NDVI products of Sentinel-3A SLSTR in monitoring agricultural drought.

1. Introduction

Agricultural drought is a natural hazard and a complex worldwide phenomenon (Wilhite and Glantz, 1985; Smith and Katz, 2013) that is closely related to water security and crop production and can even lead to significant economic losses, especially for developing countries (Wilhite, 2005; Godfray et al., 2010). Wilhite and Glantz (1985) categorized droughts into meteorological, hydrological, agricultural, and socioeconomic droughts, whose severity is influenced by their intensity, duration, spatial coverage, and local socioeconomic level. Agricultural drought usually refers to a period with declining soil moisture that influences crop production or crop failure without explicit reference to surface water resources (Mishra and Singh, 2010). As the importance of food security is increasingly being recognized, the development of agricultural drought monitoring methodologies has attracted much research interest. Over the past few decades, a large number of methods have been developed for studying agricultural drought based on precipitation, soil moisture, temperature, vegetation index, and other indicators.

Drought can be quantified by using meteorological data-based

* Corresponding authors at: Institute of Remote Sensing and Geographic Information System, School of Earth and Space Sciences, Peking University, Beijing 100871, China.
E-mail addresses: renhuazhong@pku.edu.cn (H. Ren), lyan@pku.edu.cn (L. Yan).

https://doi.org/10.1016/j.agrformet.2019.107707
Received 19 December 2018; Received in revised form 7 July 2019; Accepted 13 August 2019

indices, such as the Palmer drought severity index (Alley, 1984; Wells et al., 2004), crop moisture index (Palmer, 1968), surface water supply index (Shafer and Dezman, 1982; Valipour, 2013), and standardized precipitation index (McKee et al., 1993), and the development of those drought indices and their application in the USA have been reviewed by Heim (2002). To our knowledge, these indices use precipitation either singly or in combination with other meteorological elements. However, their applicability at local or regional scales primarily depends on the density and spatial distribution of the ground station networks (Rhee et al., 2010). Hazaymeh and Hassan (2016) showed that some indices can be interpolated or via reanalysis, like SPEI (Standardized Precipitation Evapotranspiration Index, Vicente-Serrano et al., 2010), and used to assess meteorological drought, but they have the problem of low spatial resolution. Furthermore, these indices also show deficiencies in near-real-time drought monitoring and in helping farmers and governments, especially those in large-scale regions and areas with sparse stations, in making crucial decisions (Unganai and Kogan, 1998; Rhee et al., 2010; Liang et al., 2012; Son et al., 2012; Sánchez et al., 2018).

With the development of satellite remote sensing technology, several studies have applied remote sensing data (e.g. multispectral, thermal infrared, or microwave data) to monitor large-scale drought (Kogan, 1995; McVicar and Jupp, 2002; Hao et al., 2017). Satellite remote sensing provides a synoptic view of the land and a spatial context for measuring the impacts of drought. This technique has also been proven to be a valuable source of timely, spatially continuous data that can facilitate the monitoring of vegetation dynamics over large areas. For instance, the normalized difference vegetation index (NDVI) calculated from remote sensing images has been widely used to monitor drought (e.g. Henricksen and Durkin, 1986; Peters et al., 2002; Klisch and Atzberger, 2016) because the value of this index can be used to separate vegetation from its soil background as well as provide valuable information related to vegetation health (Pettorelli et al., 2005). Kogan (1995) developed a vegetation condition index (VCI) that detects drought based on scaled NDVI. However, NDVI alone may not able to identify vegetation drought effectively (Heim, 2002) because many factors, such as land cover change and pest infestation, can lead to an NDVI anomaly similar to that caused by drought. The precipitation and soil moisture datasets derived from microwave satellite sensors have also been used for monitoring droughts (Sahoo et al., 2015; Liu et al., 2017). One of the key parameters in the physics of land surface processes at the local and global scales, the land surface temperature (LST) derived from satellite observations has been used singly or in combination with NDVI to monitor drought (Kogan, 1995; Karnieli et al., 2010). Other remote sensing indices have also been proposed for the same purpose, including the normalized difference water index (NDWI; Gao, 1996), normalized difference drought index (NDDI; Gu et al., 2007), vegetation temperature condition index (VTCI; e.g. Wang et al., 2001; Wan et al., 2004; Patel et al., 2012), temperature-vegetation dryness index (TVDI; Sandholt et al., 2002), and microwave integrated drought index (MIDI; Zhang and Jia, 2013). Both the VTCI and TVDI are based on the LST-NDVI scattering space.

The Sea and Land Surface Temperature Radiometer (SLSTR) onboard the Sentinel 3A of the European Space Agency (ESA) is a visible and infrared radiometer used for ocean and land monitoring. Launched on February 16, 2016, Sentinel-3A flies at an altitude of 814.5 km at a near-polar, sun-synchronous orbit with a descending node equatorial crossing at 10:00 h of the mean local solar time (Donlon et al., 2012). SLSTR observes the global surface in nine bands, of which three are in visible/NIR ranges (VNIR, centered at 0.550, 0.659, and 0.865 μm), three are in short wave infrared ranges (SWIR, centered at 1.375, 1.610, and 2.25 μm), and three are in middle and thermal infrared ranges (MIR/TIR, centered at 3.74, 10.85, and 12.0 μm). Both VNIR and SWIR images are captured at a resolution of 0.5 km, while both MIR and TIR images are captured at a resolution of 1 km. Given that VNIR and SWIR images can be used to calculate various vegetation (e.g., NDVI and Enhanced Vegetation Index, EVI) and water indices (e.g., NDWI) while TIR images are suitable for estimating LST, it is hypothesized that SLSTR observations have potential to monitor agricultural drought. This potential has not been previously evaluated and reported in the literature. This paper evaluates the VTCI drought monitoring index derived from Sentinel-3A SLSTR and compares these values against those obtained from the MODIS instrument. MODIS products have previously been widely used for monitoring drought (e.g. Wan et al., 2004; Gu et al., 2007; Son et al., 2012; Klisch and Atzberger, 2016). The objectives of this paper are (1) to analyze the LST-NDVI correlation under different vegetation growth conditions using MODIS data, (2) using the results derived from objective 1, investigate the performance of Sentinel-3A SLSTR data for agricultural drought monitoring, and (3) to evaluate the results by comparing with MODIS VTCI. The paper is organized as follows. Section 2 describes the study area and data in detail, Section 3 presents the LST-NDVI correlation analysis and evaluates the VTCI method based on SLSTR images, Section 4 presents the drought monitoring and validation results obtained in Hetao Plain, and Section 5 discusses the main findings and concludes the paper.

2. Study area and data

2.1. Hetao Plain

The Hetao Plain in Inner Mongolia of Northwest China is selected as the study area because of its small annual precipitation and high drought frequency. The Hetao Plain is a typical sediment-filled basin in Northwest China located near the north of the Yellow River and Kubuqi Desert on the eastern fringe of the Ulan Buh Desert (Fig. 1). This study area has an arid climate with an average annual precipitation ranging from 130 mm to 220 mm that mainly falls between July and September. The annual evapotranspiration in this area ranges approximately from 2000 mm to 2500 mm (Guo et al., 2008), which is much larger than the average annual precipitation. Due to a lack of water resources (Xu et al., 2010), some artificial drainage ditches have been built to divert irrigation water from the Yellow River at the western tip of the Hetao Plain to the Wuliangsuhai Lake, which then drains its excess water into the Yellow River (Guo et al., 2008). With its well-irrigated conditions, the Hetao Plain is considered one of the oldest and most important irrigated agriculture districts in China. Several types of crops, including corn, wheat, rape, and sunflower, are planted within approximately 2,500,000 ha of the plain with an annual crop production of nearly 2.5 million tonnes.

The majority of the Hetao Plain is cultivated. Fig. 2 shows a land cover map of the Hetao Plain from 30-meter GlobalLand cover data product (Chen et al., 2014, 2017). To monitor agricultural drought

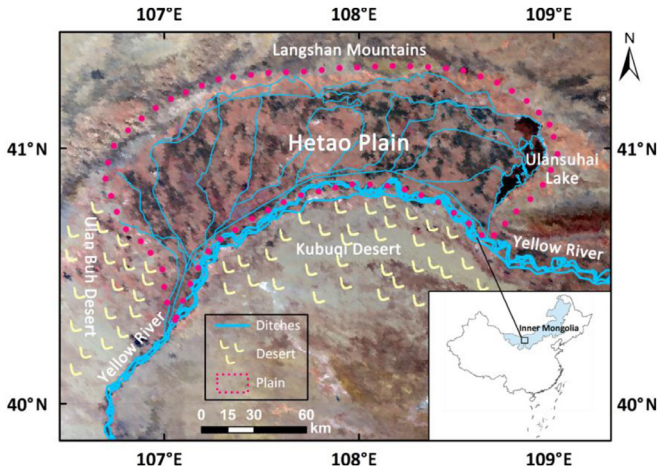

Fig. 1. Map and location of the Hetao Plain.

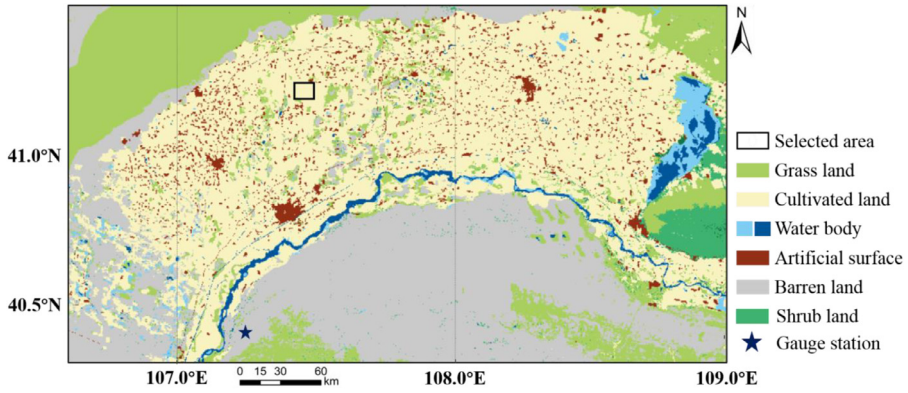

Fig. 2. Land cover map of the Hetao Plain (modified from Chen et al., 2017, available at http://www.globallandcover.com/GLC30Download/index.aspx).

based on empirical LST-NDVI relationships, the correlation between LST and NDVI must be analyzed at different periods. Therefore, we selected a representative sample with a homogeneous, stable, and cultivated land cover (black box in Fig. 2) to derive the correlation coefficients from simple linear regressions between LST and NDVI.

2.2. Image data

To calculate VTCI, the LST products of SLSTR were downloaded from ESA (https://sentinel.esa.int/). These products were generated by using a split-window algorithm that works similarly as the LST retrieval method for Advanced Along Track Scanning Radiometer (AATSR) images (Ghent et al., 2017). The corresponding NDVI was calculated from the ground reflectance of the SLSTR red and NIR bands after atmospheric correction by using the atmospheric radiative transfer code 6S (Second Simulation of the Satellite Signal in the Solar Spectrum) and the MODIS aerosol product (MOD04_L2) from the Earth Observing System Data and Information System (https://earthdata.nasa.gov/). Three clear-sky images captured in three dates of the year 2017 (July 28, DOY (day of year, Julian Day) 209; August 12, DOY 224; and August 18, DOY 230) over the study area were selected. These dates correspond to the summer growing period and occurred during a time where rainfall, obtained from the China Meteorological Data Sharing Service System (http://data.cma.gov.cn/), was determined to be variable. The period prior to July 28 was characterized by zero rainfall. Between July 28 and August 12 (Fig. 3) there was considerable rainfall in the study area. This was followed by a period without rain. Therefore, it is hypothesized that the VTCI index should be relatively low, then increasing over the wet period and finally decreasing after the wet period.

MODIS LST (MOD11A1) and surface reflectance (MOD09GA) products were also obtained in the same three dates to verify the agricultural drought results obtained by SLSTR. MODIS NDVI was computed from the surface reflectance of the red and NIR bands involved in the MOD09GA product. To investigate the correlations between LST and NDVI and to verify the availability of VTCI for monitoring agricultural drought in the study area, we downloaded 7.5 years' (January 2011 to June 2018) worth of MODIS LST and NDVI products (MOD11A2 and MOD13A2) with 8-day and 16-day composite data, respectively.

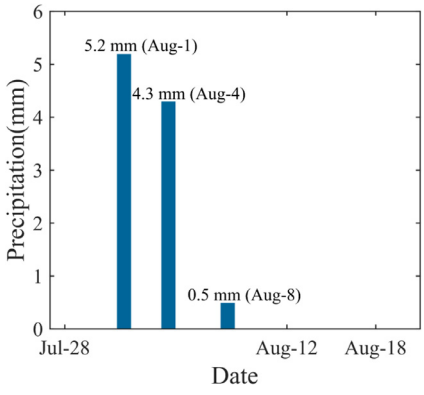

Fig. 3. Precipitation in the study area from July 28 to August 18.

3. Agricultural drought monitoring method

3.1. LST-NDVI correlation analysis

It was necessary to determine the relationship between NDVI and LST using a comparable satellite data product, in this case MODIS, to confirm the behavior of the equivalent products derived from Sentinel-3A SLSTR. Fig. 4 shows the averages and the mean plus or minus a standard deviation (shaded area) of LST and NDVI in the study area (Fig. 2) from MODIS between 2011 and 2018. Both higher values of NDVI and LST recorded during the summer growing season (from June to September) and lower values recorded during winter. However, the increase in NDVI demonstrated a hysteretic trend in contrast to LST, which fitted the trend of the vegetation growth process (Sun and Kafatos, 2007).

Based on the results presented in Fig. 4, the average of two adjacent LSTs (MOD11A2 product) was calculated to correspond to the NDVI (MOD13A2 product) because the former provides an average LST of 8-day compositing period while the latter provides an NDVI with a 16-day compositing period. The LST-NDVI correlations in each pair of observations from 2011 to 2018 were then calculated and their correlation coefficients are presented in Fig. 5. The seasonal variability of the LST and NDVI correlation coefficients indicate that different climatic variables govern their correlations at different times of the year. Specifically, a negative correlation was observed during the warm season (in April and summer season) when sufficient solar radiation is available for the crops and soil moisture or precipitation acts as the primary stress factor for vegetation growth. In April, there a negative correlation is observed, because the spring drought has frequently occurred in Hetao plain. By contrast, a positive correlation was observed during winter and the early spring period because the amount of solar energy that supports photosynthesis decreases and temperature limits the growth of plants, thereby leading to sparse vegetation and, at certain times, snow cover. Therefore, these drought indices, which are based on LST-NDVI relationships, should only be used in periods where crop growth is likely to occur, referred to as warm seasons. This is when negative correlations are observed, that is, when water (instead of energy) is the primary factor that limits vegetation growth. In Section 4.1, three clear-sky Sentinel-3A SLSTR data were obtained between July and August (DOY 182 and DOY 243) from the study area to analyze

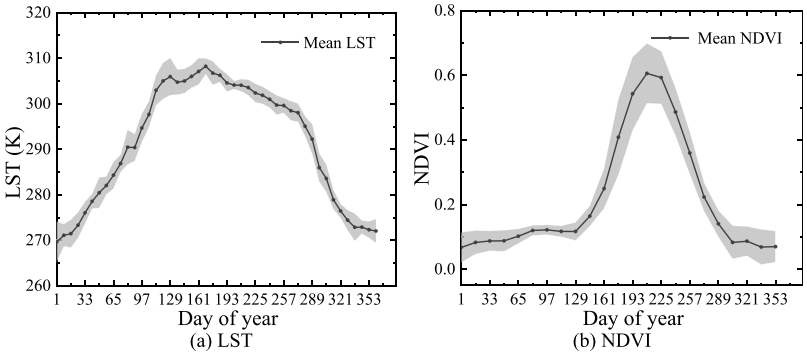

Fig. 4. Annual variation of (a) MODIS LST and (b) NDVI in the study area from 2011 to 2018.

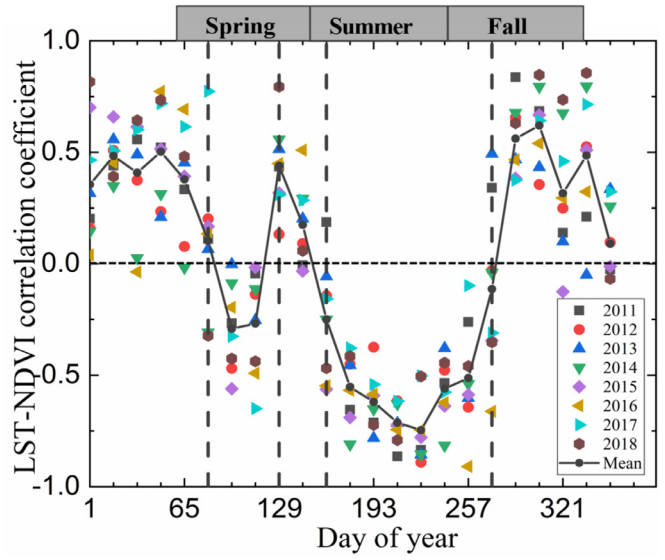

Fig. 5. The annual variation of LST and NDVI correlations from 2011 to 2018.

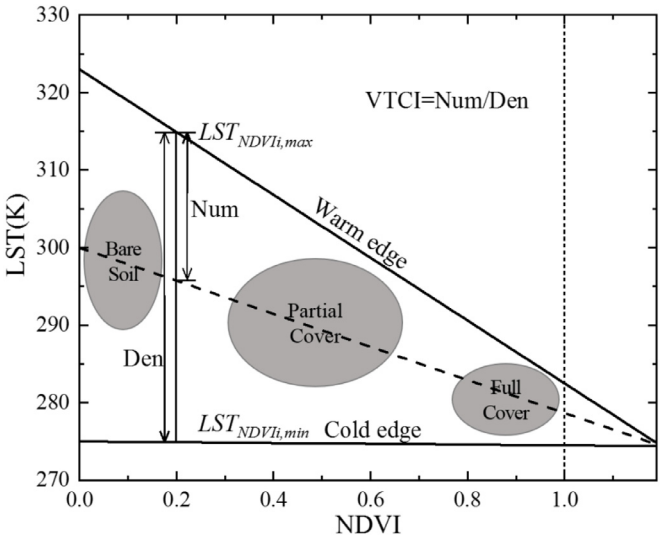

Fig. 6. The LST-NDVI triangle space and VTCI. The vertical dashed line denotes the maximum NDVI value (about 1.0). Modified from Wan et al. (2004).

agricultural drought.

3.2. The VTCI method for monitoring agricultural drought

VTCI uses the LST-NDVI scattering space technique (illustrated in Fig. 6; Wan et al., 2004) to monitor agricultural drought. In this LST-NDVI space, some pixels have similar NDVI values yet different LSTs. Therefore, a maximum LST and a minimum LST is available for each NDVI value in theory. The maximum LSTs vary along with NDVIs and can be linearly regressed as $LST_{NDVI_i,max} = a + b \cdot NDVI_i$. The regression line is called the warm or dry edge of the triangle (Fig. 6), while the regression line between the minimum LST and NDVI ($LST_{NDVI_i,min} = a' + b' \cdot NDVI_i$) is called the cold or wet edge. VTCI can be defined as

$$VTCI = \frac{LST_{NDVI_i,max} - LST_{NDVI_i}}{LST_{NDVI_i,max} - LST_{NDVI_i,min}}, \quad (1)$$

where, $LST_{NDVI_i,max} = a + b \cdot NDVI_i$ and $LST_{NDVI_i,min} = a' + b' \cdot NDVI_i$.

In Eq. (1), the denominator is computed as the difference between the maximum ($LST_{NDVI_i,max}$) and minimum LSTs ($LST_{NDVI_i,min}$) for the specified $NDVI_i$, while the numerator is computed as the difference between the maximum and current pxel LSTs (LST_{NDVI_i}). *a, b, a′*, and *b′* are the coefficients for the linear regression which accuracies are crucial for measuring VTCI. Therefore, the region used for building the LST-NDVI triangle space must be large enough to represent the entire range of surface moisture contents from wet to dry and from bare soil to fully vegetated surface. In general, the coefficients can be estimated from the scatter plot of the LST and NDVI in the study area. The shape of the scattering space is normally triangular or trapezoidal if the study area is large enough to provide a wide range of NDVI and surface moisture conditions (Han et al., 2010; Gillies et al., 1997; Wang et al., 2001). In other words, VTCI can be used in water-limited vegetation growth conditions when LST and NDVI are negatively correlated (Section 3.1) and when the coefficients (*a, b, a′,* and *b′)* of the warm and cold edges can be determined effectively.

As stated above, $LST_{NDVI_i,max}$ is regarded as the warm or dry edge for VTCI = 0, which indicates a condition with relatively less soil moisture, corresponding to a relatively limited evaporation, and plants are considered as suffering water-stress conditions. Meanwhile, $LST_{NDVI_i,min}$ is known as the cold or wet edge for VTCI = 1, which indicates a condition with minimum water restriction or maximum transpiration for plant growth (Gillies et al., 1997; Wang et al., 2001). Therefore, a lower VTCI corresponds to a higher occurrence of drought. Unlike the TVDI that uses a constant LST_{min}, VTCI uses various $LST_{NDVI_i,min}$ for each $NDVI_i$, thereby producing better results than TVDI because the cold edges are not directly horizontal in most LST-NDVI triangle spaces. Having horizontal lines may lead to the overestimation of TVDI at low NDVI values. According to Wang et al. (2004), VTCI can be divided into five drought levels, namely, $0.0 < VTCI \leq 0.2$ (severely dry), $0.2 < VTCI \leq 0.4$ (dry), $0.4 < VTCI \leq 0.6$ (water balanced), $0.6 < VTCI \leq 0.8$ (wet), and $0.8 < VTCI \leq 1.0$ (very wet). Given that the absolute soil moisture cannot be known from this VTCI or from some similar methods, the value of VTCI can only reflect the relative level of agricultural drought.

The method proposed by Tang et al. (2010) was used to estimate the

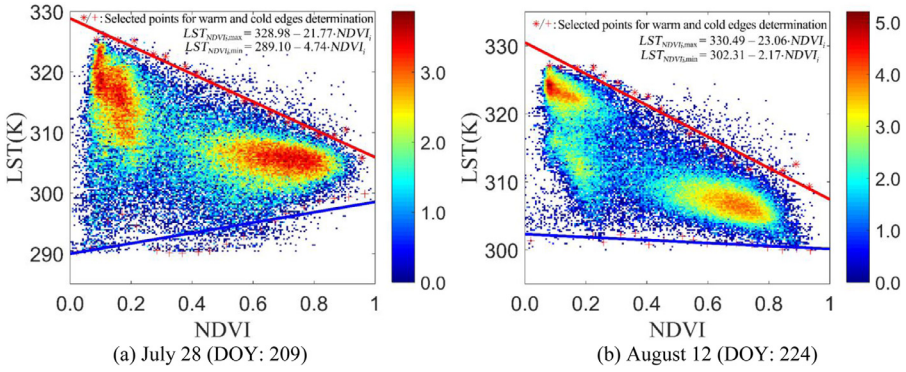

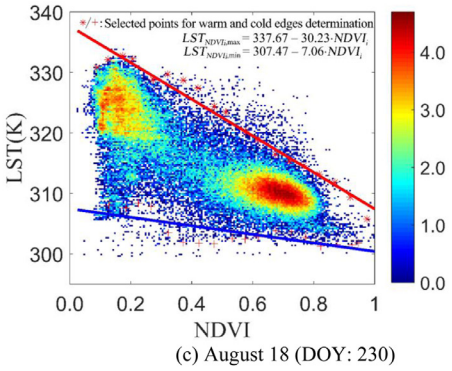

Fig. 7. The LST-NDVI triangle spaces for the Sentinel-3A SLSTR data on three dates. Both warm and cold edges are shown. The color indicates the number of observations in each bin on a logarithmic scale, growing from blue (1 observation) to red (the maximum). (For interpretation of the references to color in this figure legend, the reader is referred to the web version of this article.)

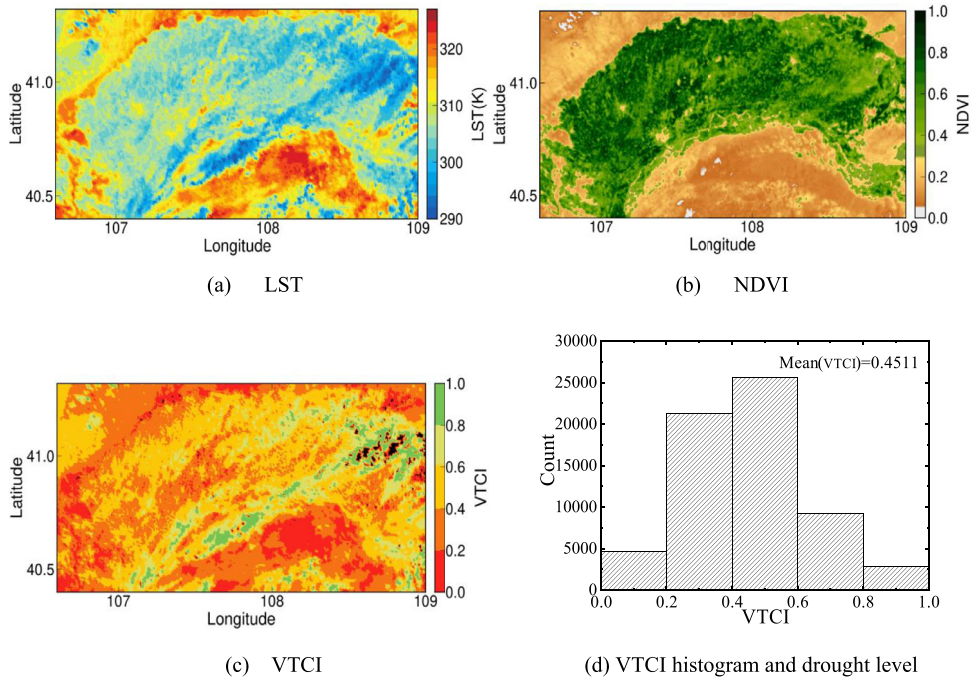

Fig. 8. The LST, NDVI, and VTCI images and the VTCI histograms of the Hetao Plain in the three dates (A, B, C).

warm and cold edges, and we made some improvements to discard the abnormal value in the initial step. For the warm edge of the triangle, all NDVIs were initially divided into 20 intervals, with each interval divided into five subintervals. The LST was regarded as abnormal and discarded if its value exceeds the average value (LST_{avg}) plus or minus three times of the standard deviation (σ) of all LSTs in a specified subinterval. Afterward, LST_{avg} and σ were recalculated as an initial state. If the maximum LST of each subinterval was less than LST_{avg} minus one σ of the LST in these five subintervals, then this subinterval was removed and a new maximum LST was selected for the same interval. The coefficients *a* and *b* of the warm edge were then computed through a linear least square regression between the remaining maximum LST values and their corresponding NDVIs, and the root-mean-square error (RMSE) of the LST regression residual was calculated afterward. For a given interval, if the maximum LST exceeds the average LST of the remaining maximum LST plus two times RMSE, then this interval will be discarded. Afterward, the coefficients *a* and *b* were recalculated until no interval can be discarded. The warm edge and its

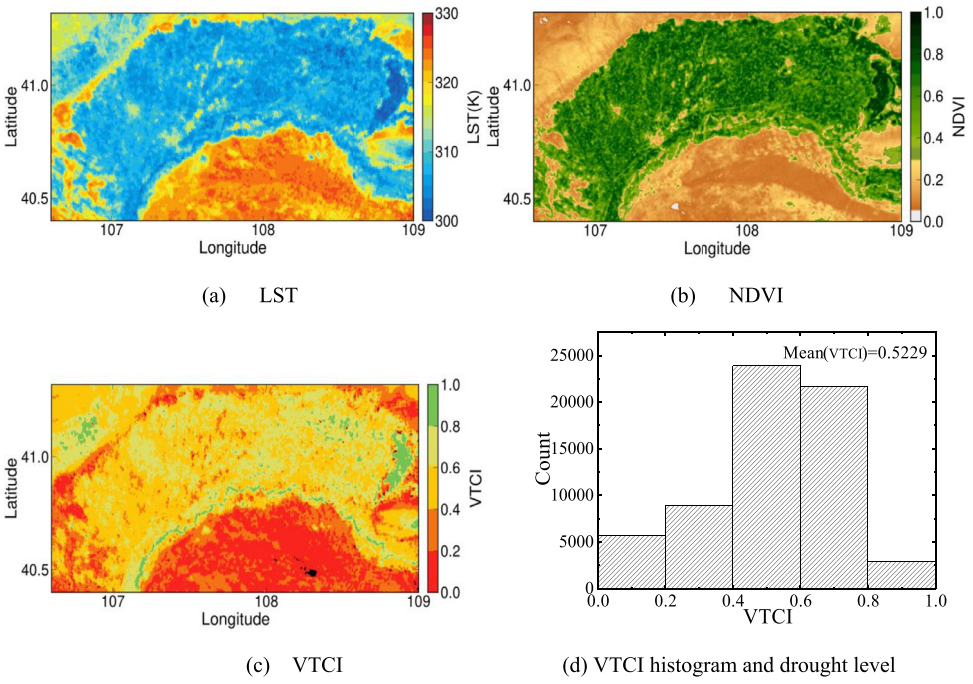

(a) LST (b) NDVI

(c) VTCI (d) VTCI histogram and drought level

(B) Results for August 12, 2017 (DOY: 224)

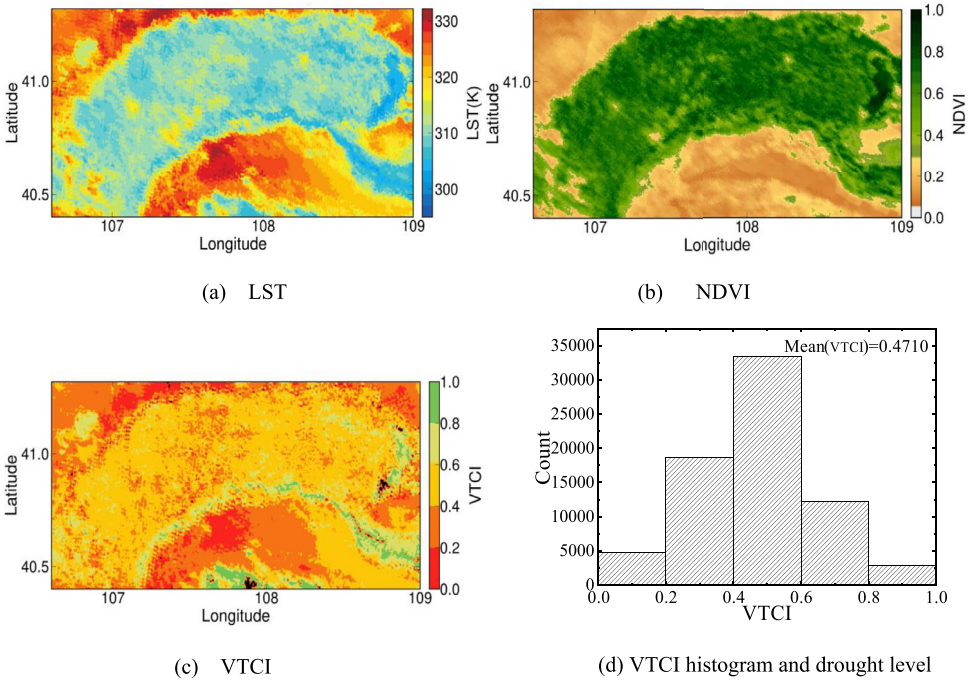

(a) LST (b) NDVI

(c) VTCI (d) VTCI histogram and drought level

(C) Results for August 18, 2017 (DOY: 230)

Fig. 8. (*continued*)

coefficients were eventually obtained through a linear regression. The cold edge was determined in a similar manner.

Fig. 7 presents the LST-NDVI triangle spaces that are obtained by plotting NDVI against LST for the SLSTR products obtained on July 28, August 12 and August 18 2017, respectively. The red asterisk and plus sign in Fig. 7 denote the warm and cold edges respectively. None of the three cold edges are horizontal, these results are in consistent with VTCI's definition. All points above the warm edge were removed from the analysis as it was determined that these were caused by non-cultivated surfaces.

4. Agricultural drought monitoring results and analysis

4.1. Temporal behavior of VTCI from Sentinel-3A SLSTR

VTCI results, derived from LST and NDVI images collected from the study area over three dates from SLSTR are presented in Fig. 8 along with their corresponding statistical histograms. To compare the changes in the VTCI of cultivated land, only the VTCIs for the pixels with NDVI larger than 0.15 were calculated. A higher drought occurrence (indicated by low VTCI) was observed in the west and south parts of the study area (Kubuqi Desert), while some areas in the east part and along

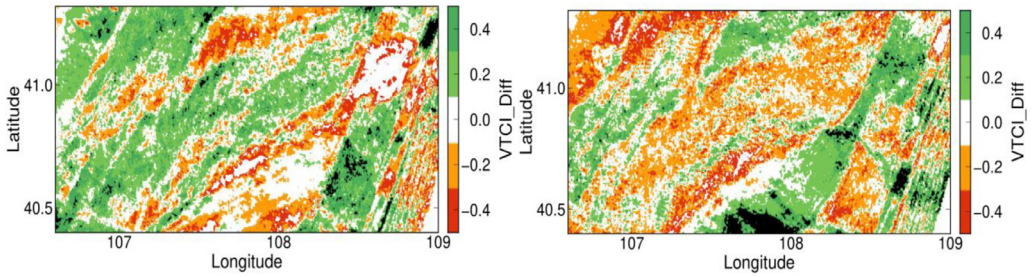

Fig. 9. Differences of VTCIs between three dates. (a) The difference of VTCIs captured on July 28 and August 12, and (b) the difference of VTCIs captured on August 12 and August 18.

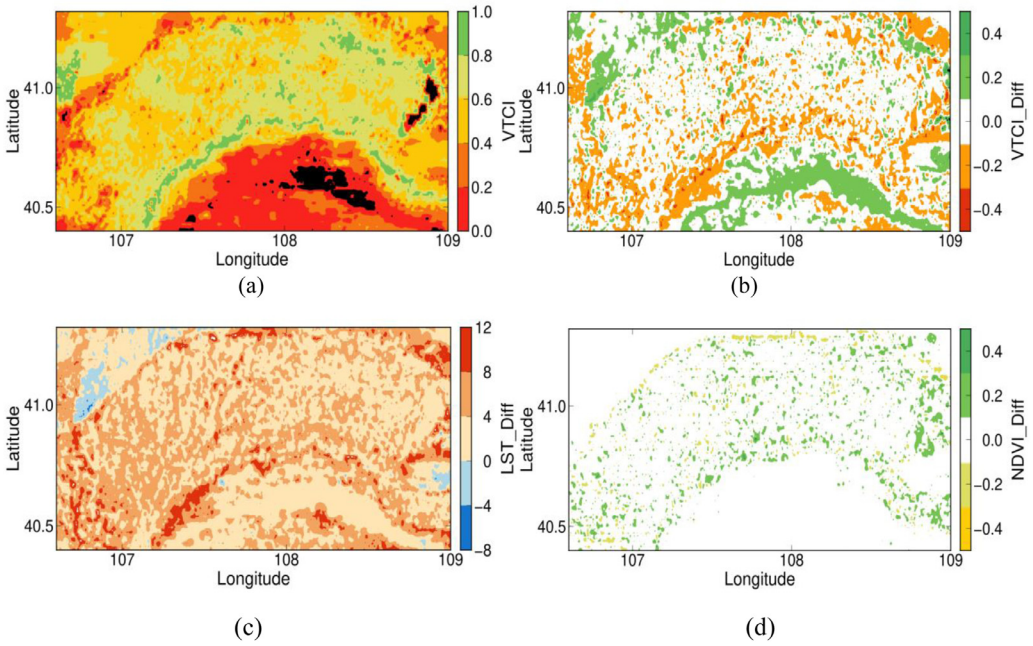

Fig. 10. (a) VTCI images of Hetao Plain captured on August 12 (DOY: 224) by MODIS observations, and the differences of (b) VTCIs, (c) LSTs, and (d) NDVIs between Sentinel-3A SLSTR and MODIS (i.e., SLSTR minus MODIS).

the Yellow River were under wet conditions (see Fig. 8(c)s). The VTCI histograms (Fig. 8(d)s) show that the average VTCI value initially increases from 0.4511 on July 28 to 0.5229 on August 12 before decreasing back to 0.4710. This result indicates that the drought level recorded on August 12 was less severe than those recorded on July 28 and August 18. This corresponds well with the precipitation data, which revealed that significant precipitation occurred in the study area between July 28 and August 12 (Fig. 3). The results also reveal that the VTCI was sensitive to rainfall and, therefore, was sensitive to both soil moisture content and variation, and can be used for monitoring agricultural drought in the study area.

We compared the VTCI images obtained in three separate dates and present the results in Fig. 9, in which (a) presents the difference in the VTCIs recorded on July 28 and August 12. Given that several precipitations occurred in the study area between August 12 and August 18, the drought severity should decline. Fig. 9(a) also shows that the VTCI difference value (VTCI in August 12 minus VTCI in July 28) was positive in most areas, thereby suggesting that the drought severity has weakened. However, in the south of Hetao Plain, the VTCI difference value decreased perhaps due to the influence of the high temperature and dry winds driven from the south desert area.

As shown in Fig. 9(b), the difference value (VTCI on August 18 minus VTCI on August 12) was negative in most areas, thereby suggesting that the drought severity increased in these areas. Fig. 3 reveals that no precipitation has occurred between August 12 and August 18 and that evapotranspiration has reduced the water content in both the soil and vegetation. The changes in the VTCI recorded in the three selected dates indicated that the agricultural drought monitoring results conformed to the actual observations.

4.2. Comparison using MODIS LST and surface reflectance products

MODIS products have been widely used in drought monitoring (Wan et al., 2004; Gu et al., 2007; Son et al., 2012; Klisch and Atzberger, 2016). Therefore, we used the MODIS LST product (MOD11A1) and NDVI (from the surface reflectance product MOD09GA) to validate the agricultural drought monitoring results obtained from the SLSTR images. The ground surface reflectance for bands 1 (620–670 nm) and 2 (841–876 nm) from MOD09GA were used to compute NDVI. The LST-NDVI triangle space was then created following the aforementioned procedures before calculating VTCI. Taking the result of August 12 as an example, Fig. 10(a) presents the VTCI image of MODIS observations, and figures (b), (c) and (d) show the differences of TVCI, LST and NDVI between Sentinel-3A SLSTR and MODIS. Since in that day the local overpassing time of MODIS and SLSTR imageries were around 10:18 am and 11:34 am, respectively, all of Fig. 10(b), (c) and (d) were the results of the SLSTR minus MODIS.

Fig. 10 shows that there are areas where the VTCI from MODIS and Sentinel-3A SLSTR are similar but also where there are differences. In Fig. 10(b), most of the difference values between two types of satellite

data in the cultivated land ranged from −0.1 to 0.1. However, the non-cultivated land (e.g., Yellow River, Kubuqi Desert south of Hetao Plain, and some artificial land in the plain) showed large difference values. In Fig. 10(c), it is seen that the LST difference was more pronounced. This is thought to be because the overpass time between two sensors differed by around 90 min, thereby producing a temperature difference in the period of warming in the morning. Furthermore, different LST retrieval algorithms were applied between the MODIS LST product and the Sentinel-3A SLSTR LST product, thereby possibly explaining the LST difference between MODIS and SLSTR and the differences in their VTCIs. However, the VTCI difference was not orders of magnitude apart in cultivated land, thereby suggesting that the Sentinel-3A SLSTR can be used to monitor drought in cultivated land alongside MODIS derived VTCI. Given that the value of VTCI was effective and sensitive to rainfall as explained in Sections 4.1 and 4.2, this index may be considered as a future drought monitoring indicator that can be further used along-side MODIS (with a note of caution about the overpass times) or on its own.

5. Discussion and conclusion

When combined with the LST and NDVI retrieved from satellite data, VTCI may provide more valuable information for agricultural drought monitoring, especially in large-scale areas and regions with insufficient ground monitoring stations or infrastructure. The index is also sensitive to rainfall and may effectively provide near-time drought information. This work combined the VTCI obtained from Sentinel-3A SLSTR LST with NDVI to monitor agricultural drought in the Hetao Plain and obtained reasonable results. MODIS products, which have been widely applied for monitoring agricultural drought, were also used to evaluate the results. A comparison between VTCI values derived from different satellites show some differences, thought to be as a result of different overpass times acquiring different LST estimates, but there is consistency between products that support the continued development of VTCI from Sentinel-3A SLSTR products. A more thorough validation exercise is needed by comparing VTCI values with soil moisture data, such as the soil moisture active passive (SMAP; Entekhabi et al., 2010) and the in-situ measured soil moisture data. As the objective of this paper is to determine the potential use of VTCI from the new Sentinel-3 satellite, this has been designated as future work. We further plan to investigate the temporal evolution of VTCI parameters by using multi-temporal Sentinel-3A SLSTR data for the Hetao Plain and other agricultural regions, and to improve VTCI by considering similar vegetation indices, like the NDWI derived from SLSTR. It has been proposed that the NDWI is less sensitive to atmospheric scattering effects, and more sensitive to changes in liquid water content of vegetation canopies than NDVI (Gao, 1996).

The VTCI derived from LST and NDVI in Sentinel-3A SLSTR products is applied for the first time to monitor agricultural drought in the Hetao Plain of Inner Mongolia. The LST–NDVI triangle space, warm edge, and cold edge are well-defined over three separate dates in the summer growing season. Analyses of VTCI data obtained over three dates reveal a high drought occurrence in the west and south areas of the plain. However, some areas in the east area and along the Yellow River were experiencing wetter conditions which were detected by the VTCI data. Using MODIS data, the VTCI has been shown to be useful in summer months when negative correlations between LST and NDVI are observed, that is, when water-not energy-is primary factor for limiting vegetation growth. The VTCI indicator was also found to be sensitive to rainfall. The comparison of the results from MODIS and SLSTR revealed a high consistency in their spatial distribution in cultivated areas. These findings show that Sentinel-3A SLSTR products can be used to monitor agricultural drought the same way as MODIS products, but that they cannot be compared directly due to overpass time differences. The observation that VTCI responded quickly to a known precipitation event was encouraging if the product is developed further as a drought monitoring indicator.

Acknowledgments

This work was supported by the UK government for supporting the Agri-Tech in China Newton Network+ (ATCNN) Small Project Award “Using Sentinel data for drought monitoring” (No. SM007), and National Natural Science Foundation of China (No. 41771369).

References

Alley, W.M., 1984. The palmer drought severity index: limitations and assumptions. J. Appl. Meteorol. 23 (23), 1100–1109.
Chen, J., Ban, Y., Li, S., 2014. China: open access to earth land-cover map. Nature 514 (7523), 434. https://doi.org/10.1038/514434c.
Chen, J., Liao, A., Chen, J., Peng, S., Chen, L., Zhang, H., 2017. 30-meter global lands cover data product – globe land30. Geomat. World 24 (1), 1–8 [In Chinese with English abstract].
Donlon, C., Berruti, B., Buongiorno, A., Ferreira, M.H., Féménias, P., Frerick, J., et al., 2012. The global monitoring for environment and security (GMES) Sentinel-3 mission. Remote Sens. Environ. 120 (6), 37–57.
Gao, B.C., 1996. NDWI-A normalized difference water index for remote sensing of vegetation liquid water from space. Remote Sens. Environ. 58 (3), 257–266.
Ghent, D.J., Corlett, G.K., Göttsche, F.M., Remedios, J.J., 2017. Global land surface temperature from the along-track scanning radiometers. J. Geophys. Res. 122 (22), 12167–12193.
Gillies, R.R., Kustas, W.P., Humes, K.S., 1997. A verification of the ``triangle" method for obtaining surface soil water content and energy fluxes from remote measurements of the normalized difference vegetation index (NDVI) and surface. Int. J. Remote Sens. 18 (15), 3145–3166.
Godfray, H.C.J., Beddington, J.R., Crute, I.R., Haddad, L., Lawrence, D., et al., 2010. Food security: the challenge of feeding 9 billion people. Science 327 (5967), 812–818. https://doi.org/10.1126/science.1185383.
Gu, Y., Brown, J.F., Verdin, J.P., Wardlow, B., 2007. A five year analysis of MODIS NDVI and NDWI for grassland drought assessment over the central great plains of the United States. Geophys. Res. Lett. 34 (6). https://doi.org/10.1029/2006GL029127.
Guo, H., Yang, S., Tang, X., Li, Y., Shen, Z., 2008. Groundwater geochemistry and its implications for arsenic mobilization in shallow aquifers of the Hetao basin, Inner Mongolia. Sci. Total Environ. 393 (1), 131–144.
Hao, Z., Yuan, X., Xia, Y., Hao, F., Singh, V.P., 2017. An overview of drought monitoring and prediction systems at regional and global scales. Bull. Am. Meteorol. Soc. 98 (9), 1879–1896.
Han, Y., Wang, Y., Zhao, Y., 2010. Estimating soil moisture conditions of the greater Changbai Mountains by land surface temperature and NDVI. IEEE Trans. Geosci. Remote Sens. 48 (6), 2509–2515.
Hazaymeh, K., Hassan, Q.K., 2016. Remote sensing of agricultural drought monitoring: a state of art review. Aims Environ. Sci. 3 (4), 604–630.
Heim, R.R.J., 2002. A review of twentieth-century drought indices used in the United States. Bull. Am. Meteorol. Soc. 83 (8), 1149–1165.
Henricksen, B.L., Durkin, J.W., 1986. Growing period and drought early warning in Africa using satellite data. Int. J. Remote Sens. 7 (11), 1583–1608.
Karnieli, A., Agam, N., Pinker, R.T., Anderson, M., Imhoff, M.L., Gutman, G.G., et al., 2010. Use of NDVI and land surface temperature for drought assessment: merits and limitations. J. Clim. 23 (3), 618–633.
Entekhabi, D., Njoku, E.G., O'Neill, P.E., Kellogg, K.H., Crow, W.T., Edelstein, W.N., et al., 2010. The soil moisture active passive (SMAP) mission. Proc. IEEE 98 (5), 704–716.
Klisch, A., Atzberger, C., 2016. Operational drought monitoring in Kenya using MODIS NDVI time series. Remote Sens. 8 (4), 267.
Kogan, F.N., 1995. Application of vegetation index and brightness temperature for drought detection. Adv. Space Res. 15 (11), 91–100.
Liang, S.L., Li, X.W., Wang, J.D., 2012. Advanced Remote Sensing: Terrestrial Information Extraction and Applications. Academic Press.
Liu, D., Mishra, A.K., Yu, Z., Yang, C., Konapala, G., Vu, T., 2017. Performance of SMAP, AMSR-E and LAI for weekly agricultural drought forecasting over continental United States. J. Hydrol. 553, 88–104.
McKee, T.B., Doesken, N.J., Kleist, J., 1993. The relationship of drought frequency and duration to time scales. In: Proceedings of the 8th Conference of Applied Climatology, January 1993. Anaheim, CA. 17. American Meteorological Society, pp. 179–184.
McVicar, T.R., Jupp, D., 2002. Using covariates to spatially interpolate moisture availability in the Murray–Darling Basin: a novel use of remotely sensed data. Remote Sens. Environ. 79 (2), 199–212.
Mishra, A.K., Singh, V.P., 2010. A review of drought concepts. J. Hydrol. 391, 202–216.
Palmer, W.C., 1968. Keeping track of crop moisture conditions, nationwide: the new crop moisture index. Weatherwise 21 (4), 156–161.
Patel, N.R., Parida, B.R., Venus, V., Saha, S.K., Dadhwal, V.K., 2012. Analysis of agricultural drought using vegetation temperature condition index (VTCI) from Terra/MODIS satellite data. Environ. Monit. Assess. 184 (12), 7153–7163.
Peters, A.J., Walter-Shea, E.A., Ji, L., Vina, A., Hayes, M., Svoboda, M.D., 2002. Drought monitoring with NDVI-based standardized vegetation index. Photogramm. Eng. Remote Sens. 68 (1), 71–75.
Pettorelli, N., Vik, J.O., Mysterud, A., Gaillard, J.M., Tucker, C.J., Stenseth, N.C., 2005. Using the satellite-derived NDVI to assess ecological responses to environmental

change. Trends Ecol. Evol. 20 (9), 503–510.
Rhee, J., Im, J., Carbone, G.J., 2010. Monitoring agricultural drought for arid and humid regions using multi-sensor remote sensing data. Remote Sens. Environ. 114, 2875–2887.
Sánchez, N., González-Zamora, Á., Martínez-Fernández, J., Piles, M., Pablos, M., 2018. Integrated remote sensing approach to global agricultural drought monitoring. Agric. For. Meteorol. 259, 141–153.
Sahoo, A.K., Sheffield, J., Pan, M., Wood, E.F., 2015. Evaluation of the tropical rainfall measuring mission multi-satellite precipitation analysis (TMPA) for assessment of large-scale meteorological drought. Remote Sens. Environ. 159, 181–193.
Sandholt, I., Rasmussen, K., Andersen, J., 2002. A simple interpretation of the surface temperature/vegetation index space for assessment of surface moisture status. Remote Sens. Environ. 79 (2), 213–224.
Shafer, B.A., Dezman, L.E., 1982. Development of a surface water supply index (SWSI) to assess the severity of drought conditions in snowpack runoff areas. In: Western Snow Conference. Washington. 1982. pp. 164–175.
Smith, A.B., Katz, R.W., 2013. Us billion-dollar weather and climate disasters: data sources, trends, accuracy and biases. Nat. Hazards 67 (2), 387–410.
Son, N.T., Chen, C.F., Chen, C.R., Chang, L.Y., Minh, V.Q., 2012. Monitoring agricultural drought in the lower Mekong basin using MODIS NDVI and land surface temperature data. Int. J. Appl. Earth Observ. Geoform. 18 (1), 417–427.
Sun, D., Kafatos, M., 2007. Note on the NDVI-LST relationship and the use of temperature-related drought indices over North America. Geophys. Res. Lett. 34, L24406. https://doi.org/10.1029/2007GL031485.
Tang, R.L., Li, Z.L., Tang, B.H., 2010. An application of the Ts-VI triangle method with enhanced edges determination for evapotranspiration estimation from MODIS data in arid and semi-arid regions: implementation and validation. Remote Sens. Environ. 114 (3), 540–551.
Unganai, L.S., Kogan, F.N., 1998. Drought monitoring and corn yield estimation in Southern Africa from AVHRR data. Remote Sens. Environ. 63, 219–232.
Valipour, M., 2013. Use of surface water supply index to assessing of water resources management in Colorado and Oregon, US. Adv. Agric. Sci. Eng. Res. 3 (2), 631–640.
Vicente-Serrano, S., Beguería, S., López-Moreno, J.I., 2010. A multiscalar drought index sensitive to global warming: the standardized precipitation evapotranspiration index. J. Clim. 23 (7), 1696–1718.
Wan, Z., Wang, P.X., Li, X.W., 2004. Using MODIS land surface temperature and normalized difference vegetation index products for monitoring drought in the Southern Great Plains in the US. Int. J. Remote Sens. 25 (1), 61–72.
Wang, C., Qi, S., Niu, Z., Wang, J., 2004. Evaluating soil moisture status in China using the temperature-vegetation dryness index (TVDI). Can. J. Remote Sens. 30 (5), 671–679.
Wang, P.X., Li, X.W., Gong, J.Y., Song, C.H., 2001. Vegetation temperature condition index and its application for drought monitoring. In: the Proceedings of International Geoscience and Remote Sensing Symposium. Sydney, Australia. pp. 141–143.
Wells, N., Goddard, S., Hayes, M.J., 2004. A self-calibrating Palmer drought severity index. J. Clim. 17 (12), 2335–2351.
Wilhite, D.A., 2005. Drought and Water Crises: Science, Technology, and Management Issues 86. CRC Press, pp. 432.
Wilhite, D.A., Glantz, M.H., 1985. Understanding: the drought phenomenon: the role of definitions. Water Int. 10 (3), 111–120.
Xu, X., Huang, G., Qu, Z., Pereira, L.S., 2010. Assessing the groundwater dynamics and impacts of water saving in the Hetao Irrigation District, Yellow River basin. Agric. Water Manag. 98 (2), 301–313.
Zhang, A., Jia, G., 2013. Monitoring meteorological drought in semiarid regions using multi-sensor microwave remote sensing data. Remote Sens. Environ. 134 (7), 12–23.